

Mg-RICH METABASALTS FROM THE SOUTHERN MUSOMA –MARA GREENSTONE BELT: POSSIBLE EVIDENCE FOR MANTLE PLUME ACTIVITY IN THE TANZANIA CRATON?

S Manya

Department of Geology, University of Dar es Salaam,
P.O. Box 35052, Dar es Salaam, TANZANIA.

Corresponding author (email: shukrani73@udsm.ac.tz), shukrani73@yahoo.com

ABSTRACT

Mg-rich metabasalts from the Simba Sirori to Majimoto segment of the southern Musoma-Mara greenstone belt are the most magnesian lavas reported in the Archaean Tanzania Craton. The lavas yielded a Sm-Nd isochron age of 2768 ± 38 Ma (MSWD = 1.2) and corresponding $\epsilon Nd(2.7$ Ga) values in the range of + 0.66 to + 2.81. The lavas exhibit high MgO contents of up to 16 wt %, Cr (140 – 1590 ppm), Ni (80 – 510 ppm), values which are higher than those of primitive NMORB, but are comparable with those of Archaean komatiitic basalts and modern oceanic plateau basalts. Their REE patterns range from the light REE – depleted ($La/Sm_{CN} = 0.46$) to nearly flat ($La/Sm_{CN} = 0.71 - 1.08$) and light REE enriched ($La/Sm_{CN} = 2.89$). They also show negative anomalies of Nb and Ti relative to adjacent elements in multi-element spidergrams. The samples exhibit higher Th/Nb ratios (0.10 – 1.50, mean = 0.39) than those of NMORB ($Th/Nb = 0.05$) and tend to crustal values ($Th/Nb = 0.80$).

The higher MgO contents of the samples than those of primitive NMORB requires a mantle source that can generate more magnesian lavas than the depleted mantle and a mantle plume is considered to be a viable source. Thus, the geochemical features of the Mg-rich basalts of Simba Sirori to Majimoto area can be explained by the fact that these rocks were generated by the contamination of komatiitic magmas by the felsic crust. The southern MMGB Mg-rich metabasalts provide a clue to the presence of komatiites, lavas that have not been documented in the Archaean craton of Tanzania. Such magnesian lavas are common in other cratons of the world including Barberton of South Africa, Belingwe of Zimbabwe, and Superior Province of Canada.

INTRODUCTION

Archaean greenstone belts, ranging in age from 2.8 to 2.6 Ga, form the northern part of the Tanzania Craton and occur south and east of Lake Victoria. These greenstone belts share many similarities with other worldwide greenstone belts. Such similarities include lithological association, deformation styles, grade of metamorphism and styles of mineralization (Condie 1997). Describing the lithological association of Archaean greenstone belts, Condie (1997) showed that these belts represent volcanic-dominated submarine supracrustal assemblages including ultramafic and mafic volcanic rocks, intermediate to felsic

volcanic rocks, volcanoclastic sedimentary rocks, chert and banded iron formations (BIF), carbonate, quartzite, arkose and hypabyssal intrusives.

Previous studies in the Archaean greenstone belts of Tanzania for which detailed geochemical work has been done, indicate that Fe-rich tholeiites associated with rare felsic volcanic rocks, chert and BIF occur in the Sukumaland greenstone belt (e.g. Borg and Krogh 1999, Manya 2004), intermediate to felsic volcanic rocks occur in the Kilimafedha greenstone belt (Messo 2004; Wirth *et al.* 2004), high magnesian andesites and the associated intermediate to felsic

adakitic rocks occur in the Musoma-Mara greenstone belt (Manya *et al.* 2007) but ultramafic volcanic rocks including the komatiite-basalt association have not been identified in any of the greenstone belts in the Tanzania Craton (Borg and Shackleton 1997). Their absence could be attributed to poor exposure as most of the area is covered by tertiary cover (Barth 1990) or limited systematic mapping done in the area. The absence of komatiitic volcanism, considered to have been derived from a mantle plume (Campbell *et al.* 1989), provides an evidence for non-existence of divergent tectonic processes. Thus, most of the greenstone belts in the Tanzania Craton have been interpreted to have formed at convergent margin settings (e.g. Manya 2004, Cloutier *et al.* 2005, Wirth *et al.* 2004, Manya *et al.* 2007, Mtoro *et al.* 2009).

This paper presents the geochemistry and Nd-isotopic composition of the selected high-Mg basalts some of which have komatiitic affinity from the Simba Sirori - Majimoto segment of the southern part of the Musoma-Mara greenstone belt. The data is used to compare these rocks with worldwide known komatiites and komatiitic basalts, infer their petrogenesis and tectonic setting models attributed to their formation.

Geological background

The Simba Sirori - Majimoto segment of the southern part of the Musoma-Mara greenstone belt (MMGB, Fig. 1) constitutes an eastern extension of the belt studied by Mtoro *et al.* (2009). The MMGB is among the late Archaean greenstone belts that form the northern part of the Archaean Tanzania Craton. Other Archaean greenstone belts in the northern part of the Craton are Sukumaland, Shinyanga-Malita, Kilimafedha, Nzega and Iramba-Sekenke (Borg and Shackleton 1997).

The Archaean Tanzania Craton has been divided into two contrasting terranes: a

central region of granite, granodiorite, granitic gneisses and migmatites associated with metamorphic supracrustal rocks and the second which consists of granite-greenstone terrane in northern Tanzania and western Kenya (Clifford 1970). The central part is called the Dodoman belt (Wade and Oates 1938) and is considered to be older than the northern Tanzania greenstone belts. The granite-greenstone terrane consists of greenstone sequence predominantly made of mafic volcanic rocks, felsic volcanic rocks, chert and banded iron formations (BIF), felsic tuffs, agglomerates and graphitic shales of the Nyanzian Supergroup. This greenstone sequence is unconformably overlain by coarse clastic sedimentary rocks (conglomerates, sandstones, mudstones and grits) of the Kavirondian Supergroup (Barth 1990). Thin horizons of volcanic horizons occur within the rocks of the Kavirondian Supergroup (Manya *et al.* 2006).

Recent studies in the Musoma-Mara greenstone belt (MMGB, Fig. 1) have concentrated on the geochemistry and geochronology of volcanic rocks and their associated granites on different segments of the belt. Manya *et al.* (2006) reported ages of 2676 – 2667 Ma for the entire volcano-sedimentary sequence in the MMGB from the lowermost high-Mg andesites to the dacites of the Kavirondian Supergroup. A syn-orogenic granitic intrusion event dominated by TTG is dated at ~2668 Ma whereas a younger phase of post-orogenic event dominated by K-rich potassic granites concluded the magmatic evolution of the MMGB at ~2649 Ma. Such a rapid emplacement of volcanic rocks in the northern MMGB was interpreted by Manya *et al.* (2007) in terms of a ridge subduction model in a continental convergent margin. In the Suguti area, Mtoro *et al.* (2009) reported a zircon U-Pb age of 2755 ± 1 Ma for the volcanic rocks in southern MMGB and showed that both the basalts and rhyolites were cogenetic.

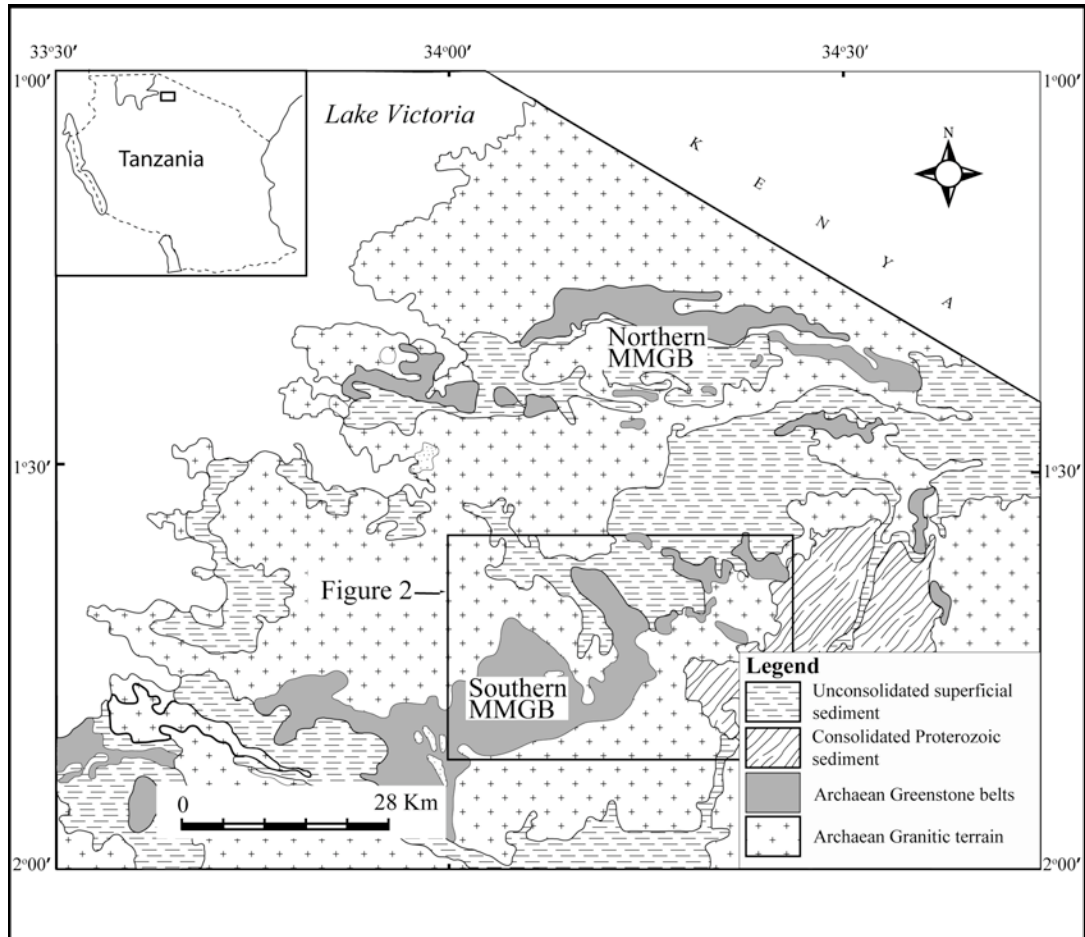


Figure 1: Geological map of the Musoma-Mara greenstone belt showing the location of the study area indicated by a frame (Modified from Borg and Shackleton 1997).

The greenstone succession of the Buhemba - Simba Sirori - Majimoto segment (Fig. 2) consists of mafic volcanic rocks at the bottom, followed by a group of interbedded felsic volcanic rocks and metasediments and a formation of rhyolites and felsites associated with intrusive porphyries at the top (Thomas and Kennedy 1965). Although regional metamorphism is of greenschist facies, the mafic volcanic rocks at Buhemba-Simba Sirori -Majimoto segment have been metamorphosed into amphibolites facies characterized by hornblende, actinolite,

epidote, feldspar and quartz mineral assemblage. The greenstone succession is intruded by syn-to post-orogenic granites as well as gabbros and dolerites.

The studied area lies closer to the Buhemba gold mine and has itself long been a centre of artisanal gold mining (Fig. 2). Gold in Simba Sirori – Majimoto area is mainly exploited as auriferous quartz reefs at the contact between granite and mafic volcanic rocks (Thomas and Kennedy 1965).

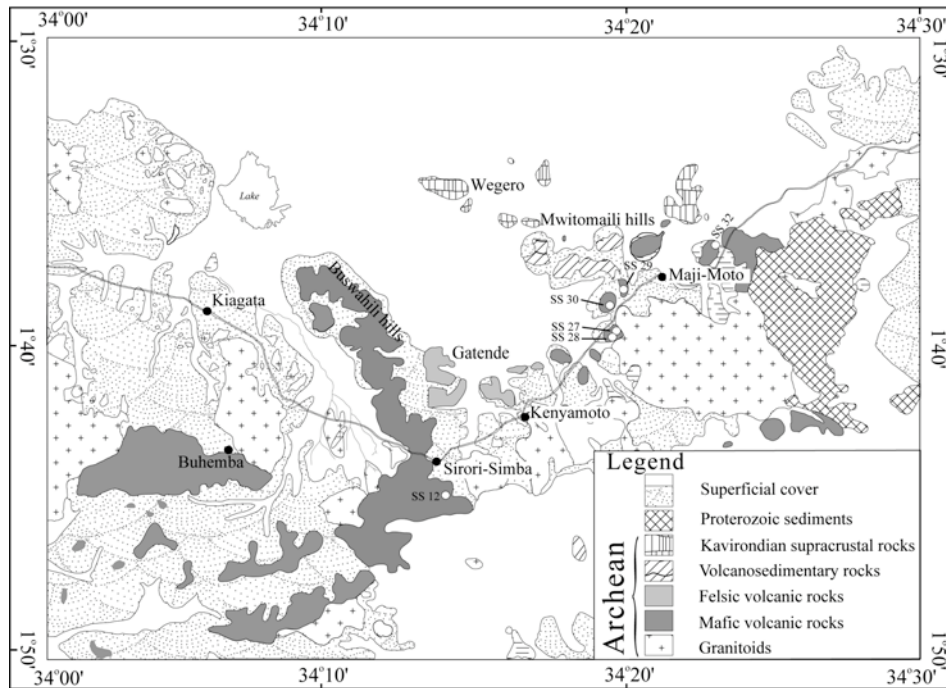


Figure 2: Geological map of the Simba Sirori – Majimoto segment of southern Musoma-Mara greenstone belt showing the sample locations (adopted from Thomas and Kennedy 1965)

MATERIALS AND METHODS

Twenty four volcanic samples were collected from the outcrop exposures in the Simba-Sirori and Majimoto segment of the southern MMGB. Sampling was dictated by the degree outcrop exposure and accessibility. All 24 samples were thin-sectioned and studied under the microscope. Petrographic description of the samples show that they are fine grained consisting principally of interlocked crystals of pyroxenes, rare olivine and plagioclase in a very fine grained groundmass. One sample (SS27) consists of radial skeletal pyroxenes and olivines, a characteristic spinifex texture (Table 1).

For geochemical analysis, the samples were pulverized to very fine powder in an agate

mill at the Southern and Eastern Africa Mineral Centre (SEAMIC) laboratories, Dar es Salaam. The samples were subsequently analyzed for major and trace elements at the Activation Laboratories of Ontario, Canada and the method is similar to that reported in Manya (2011). Precision and accuracy as deduced from replicate analyses of the BIR-1 and W2 standards are 5-10 %. The analytical reproducibility deduced from replicate analyses of the samples is better than 8% for most trace elements.

Six samples were also analysed for Sm-Nd isotopic compositions as well as Sm and Nd concentrations using a Triton-MC Thermal Ionization Mass Spectrometer at the same laboratories using the method reported in Manya (2011). Total blanks are 0.1 - 0.2 ng

for Sm and 0.1 - 0.5 ng for Nd and are negligible. The accuracy of the Sm and Nd analyses is $\pm 0.5\%$ corresponding to errors in the $^{147}\text{Sm}/^{144}\text{Nd}$ ratios of $\pm 0.5\%$ (2σ). The $^{143}\text{Nd}/^{144}\text{Nd}$ ratios are calculated relative to the value of 0.511860 for the La Jolla standard.

During the period of analysis the weighted average of 10 La Jolla Nd-standard runs yielded 0.511872 ± 15 (2σ) for $^{143}\text{Nd}/^{144}\text{Nd}$, using a $^{146}\text{Nd}/^{144}\text{Nd}$ value of 0.7219 for normalization.

Table 1: Location and Petrographic description of the Simba Sirori - Majimoto segment Mg-rich metabasalts

Sample	Location	Petrographic description
SS 12	0637055 E / 9806865 N	Fine-grained sample predominantly consisting of plagioclase and pyroxene, minor hornblende and olivine in a very fine groundmass. Other trace phases are opaque minerals and epidote
SS 27	0647237 E / 9816593 N	Sample consisting of radial skeletal pyroxene and olivine (spinfex texture) indicative of crystallization from a rapidly cooling magma
SS 28	0647237 E / 9816593 N	Sample consisting of subhedral to anhedral pyroxene, plagioclase and olivine. Some pyroxenes form dendritic pattern and olivine shows slight alteration
SS 29	0647583 E / 9818518 N	Fine-grained sample consisting of subhedral to anhedral crystals of pyroxene and plagioclase set in a fine grained groundmass of the same composition. Chlorite occur as a minor phase
SS 30	0648425 E / 9818463 N	Sample consisting of subhedral pyroxene, plagioclase and minor olivine. Epidote and opaque minerals are minor phases
SS 32	0651009 E / 9819224 N	Sample consisting of euhedral to subhedral pyroxenes that are intergrown with plagioclase. Olivine and opaque minerals occur as minor phases.

RESULTS

Classification

The Simba Sirori – Majimoto segment volcanic rocks are composed of basalts and basaltic andesites and subordinate dacites and rhyolites and are thus bimodal. Some basalts, however, have high Mg contents (> 7 wt % and up to 16 wt %). This and the fact that some samples showed spinfex texture of komatiitic affinity have drawn the attention of the author and emphasis will be placed on these high-Mg basalts whose

chemical composition appear to be different from other volcanic rocks so far reported from the greenstone belts of the Tanzania Craton. Thus, subsequent discussion is centered on six selected high Mg- basalts whose major and trace elements as well as their Nd-isotopic composition are reported.

The volcanic samples were plotted on the Jensen cation (1976) diagram (Fig. 3) and three samples (SS12, SS27 and SS28) plotted in the field of komatiitic basalts

whereas the other three (SS29, SS30 and SS32) plotted in the field of high-Fe tholeiite basalts. Komatiite (BW 272) and komatiitic basalt (BX108) samples from Belingwe greenstone belt, Zimbabwe reported by Shimizu *et al.* (2005) and those from the Ball assemblage of northern Superior Province greenstone belt, Canada (NDC87 – 01C and NDC87 – 12B) reported by Hollings *et al.* (1999) were plotted for comparison. All these plot in the field of

komatiitic basalts with the komatiites straddling the boundary between komatiites and komatiitic basalts (Fig. 3). These rocks have higher TiO₂ (0.62 – 1.15 wt %) contents than those of modern boninites (TiO₂ < 0.5 wt %, Smithies *et al.* 2004) and for this reason they do not have boninitic affinities and because of their high MgO concentrations are hereafter referred to as Mg-rich metabasalts.

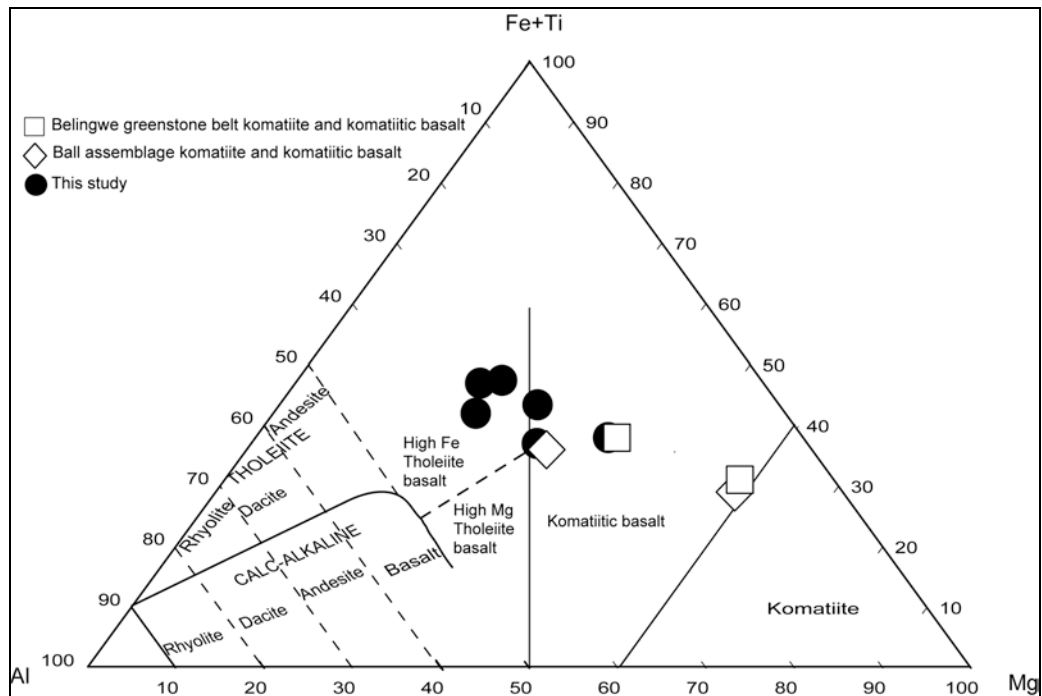


Figure 3: The Jensen (1976) cation diagram for the Simba Sirori – Majimoto segment Mg-rich metabasalts. Three samples are komatiitic basalts whereas the other three plot in the Fe-rich tholeiite basalt field. Also shown on the diagram are komatiites and komatiitic basalts from Belingwe Zimbabwe (Shimizu *et al.* 2005) and Ball assemblage Canada (Hollings *et al.* 1999).

Major and trace elements

Whole rock compositions of the Simba Sirori –Majimoto Mg-rich basalts are presented in Table 2. Their SiO₂ contents range from 48.3 to 54.5 wt%, Al₂O₃ and TiO₂ contents are 9.89 to 13.7 wt % and 0.62

– 1.15 wt % and have Al₂O₃/TiO₂ ratios of 11.9 – 18.6. Their Mg# (calculated as 100Mg/(Mg + Fe²⁺)) range from 52 to 72. Their Cr and Ni contents are 140 – 1590 ppm and 80 – 510 ppm, respectively. At the same SiO₂ value, the Simba Sirori – Majimoto

basalts have relatively higher TiO₂, Al₂O₃ and Zr contents than both Zimbabwean and Canadian komatiites and komatiitic basalts. They have, however, relatively lower MgO,

Ni and Cr contents than komatiites but compare well with komatiitic basalts from Zimbabwe and Canada (Fig. 4).

Table 2: Major (wt %) and trace (ppm) element composition of the selected Simba Sirori - Majimoto segment Mg-rich metabasalts

	Simba Sirori Mg-rich metabasalts						*Zimbabwe		*Canada	
							Komatiite	Kom Basalt	Komatiite	Kom Basalt
	SS 12	SS 27	SS 28	SS 29	SS 30	SS 32	BW272	BX 108	NDC87-01C	NDC87-12B
SiO ₂	48.8	53.9	49.3	48.4	47.21	51.6	45.51	51.04	51.85	52.08
TiO ₂	0.72	0.87	0.6	1.13	0.8	0.72	0.32	0.55	0.21	0.32
Al ₂ O ₃	12.2	10.6	9.62	13.4	12.3	13.4	6.48	11.27	5.55	8.76
Fe ₂ O ₃	10.4	12.1	12.3	13.7	14.3	11.7	10.48	9.95	11.37	11.8
MnO	0.21	0.17	0.19	0.18	0.19	0.17	0.18	0.18	0.13	0.22
MgO	11.1	10.1	15.6	7.64	8.59	7.91	25.42	11.48	25.33	14.81
CaO	11.3	8.51	8.45	11.8	12.4	9.80	6.6	8.54	5.47	10.35
Na ₂ O	1.25	2.61	1.13	2.04	1.34	2.00	0.83	2.84	0.12	0.67
K ₂ O	0.82	0.01	0.02	0.12	0.51	0.40	0.1	0.023	0.00	0.94
P ₂ O ₅	0.31	0.06	0.06	0.08	0.01	0.06	0.022	0.051	0.00	0.03
LOI	2.67	1.11	2.62	1.53	2.32	2.19	2.68	2.59	5.94	1.78
TOTAL	99.8	100	99.9	100	100.0	100.0	98.6	98.5	105.97	101.8
Mg#	68	62	72	52	54	57	83	70	82	71
Cs	5.2	0.7	1.1	0.6	1.7	1.3	0.11	0.17		
Ba	266	33	39	49	173	36	5.8	20		
Rb	88	2	6	9	56	37	1.65	0.791		
Sr	197	121	76	203	231	157	33.4	108		
Ni	350	170	510	150	100	80	1336	204	1079	253
Co	50	52	64	50	54	44			94	55
Zn	110	70	100	90	60	60				
Cu	20	40	10	60	110	80				
Cr	860	820	1590	370	140	180	2463	958	2525	1205
V	148	226	188	265	294	247			132	201
Th	4.5	0.2	0.2	0.5	0.1	0.4	0.048	0.98	0.21	0.41

Manya - Mg-rich metabasalts from the Southern Musoma –Mara greenstone belt ...

	Simba Sirori Mg-rich metabasalts						*Zimbabwe		*Canada	
							Komatiite	Kom Basalt	Komatiite	Kom Basalt
Pb	7	5	5	6	5	5	0.09	1.2		
U	0.9	0.2	0.1	0.1	0.2	0.1	0.017	0.33	0.07	0.13
Nb	3	1	1	3	1	2	0.5	1.4	0.51	1.28
Ta	1	0.3	0.2	0.5	0.3	0.4	0.032	0.1	0.04	0.1
Zr	85	40	32	72	14	42	13	34	12.1	31.7
Hf	2.1	1.1	0.9	2	0.5	1.2	0.39	1	0.39	0.91
Y	18	15	13	25	14	18	7.3	13	5.32	7.03
La	43	1.9	1.8	4.7	1	2.4	0.52	3	1.58	2.21
Ce	104	5.5	5	12.5	2.9	6.5	1.7	7	3.56	5.57
Pr	13.3	0.83	0.72	1.82	0.51	0.92	0.27	0.93	0.43	0.68
Nd	51.1	5	4	8.8	3.4	5	1.67	4.45	2.05	2.92
Sm	9.6	1.6	1.4	2.8	1.4	1.7	0.63	1.33	0.66	0.84
Eu	2.4	0.59	0.6	1.25	0.6	0.68	0.24	0.5	0.23	0.32
Gd	6.5	2.2	1.8	3.6	1.9	2.2	0.83	1.7	0.82	1.09
Tb	0.8	0.4	0.3	0.7	0.4	0.4	0.17	0.32	0.14	0.17
Dy	3.6	2.6	2.1	4.2	2.4	2.8	1.1	2.1	1.01	1.24
Ho	0.6	0.5	0.5	0.9	0.5	0.6	0.25	0.47	0.2	0.26
Er	1.6	1.7	1.3	2.6	1.5	1.9	0.68	1.3	0.58	0.8
Tm	0.23	0.25	0.2	0.4	0.22	0.28	0.11	0.21	0.08	0.12
Yb	1.4	1.6	1.3	2.5	1.4	1.8	0.74	1.4	0.65	0.73
Lu	0.21	0.22	0.2	0.39	0.23	0.28	0.11	0.2	0.1	0.12
Th/Nb	1.50	0.20	0.20	0.17	0.10	0.20	0.10	0.70	0.41	0.32
La/Sm _{CN}	2.89	0.77	0.83	1.08	0.46	0.91	0.53	1.46	1.55	1.70

* Samples from Zimbabwe (Shimizu *et al.* 2005) and Canada (Hollings *et al.* 1999) are included for comparison

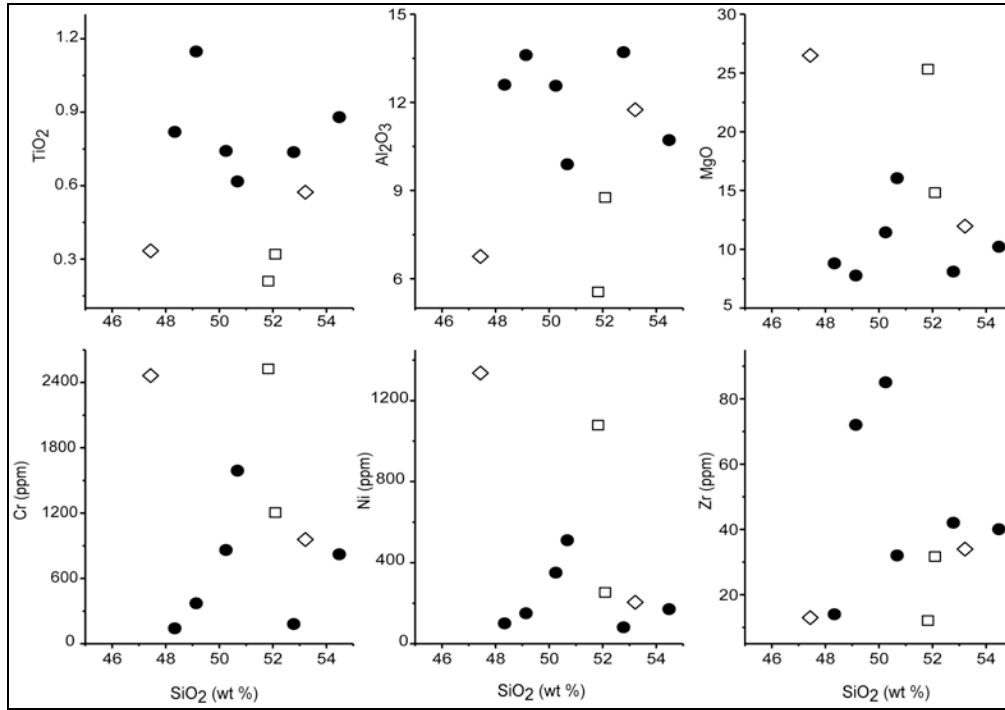


Figure 4 Harker diagrams for the Simba Sirori – Majimoto segment Mg-rich metabasalts. Symbols for Zimbabwean and Canadian komatiites and komatiitic basalts as in Fig. 3.

The samples display three kinds of Rare Earth Elements (REE) patterns (Fig. 5a). The first shows a light REE depleted signature (shown by sample SS 30 with $La/Sm_{CN} = 0.46$) which is shared by the Belingwe komatiite ($La/Sm_{CN} = 0.53$) which is slightly lower than the NMORB value ($La/Sm_{CN} = 0.61$, Sun and McDonough 1989), CN referring to chondrite normalized value. The second pattern (shown by samples SS 27, SS 28, SS29, SS32) display nearly flat REE patterns ($La/Sm_{CN} = 0.71 - 1.08$) which is similar to the tholeiitic basalts

of southern MMGB to the east of the study area reported by Mtoro *et al.* (2009). The third is displayed by sample SS 12 which show a light REE enriched pattern with $La/Sm_{CN} = 2.89$.

On primitive mantle-normalized diagrams, apart from all samples showing strong negative anomalies of Nb and minor negative Ti anomalies, samples SS 12 and SS 30 also has negative anomalies of Zr and Hf (Fig. 5b)

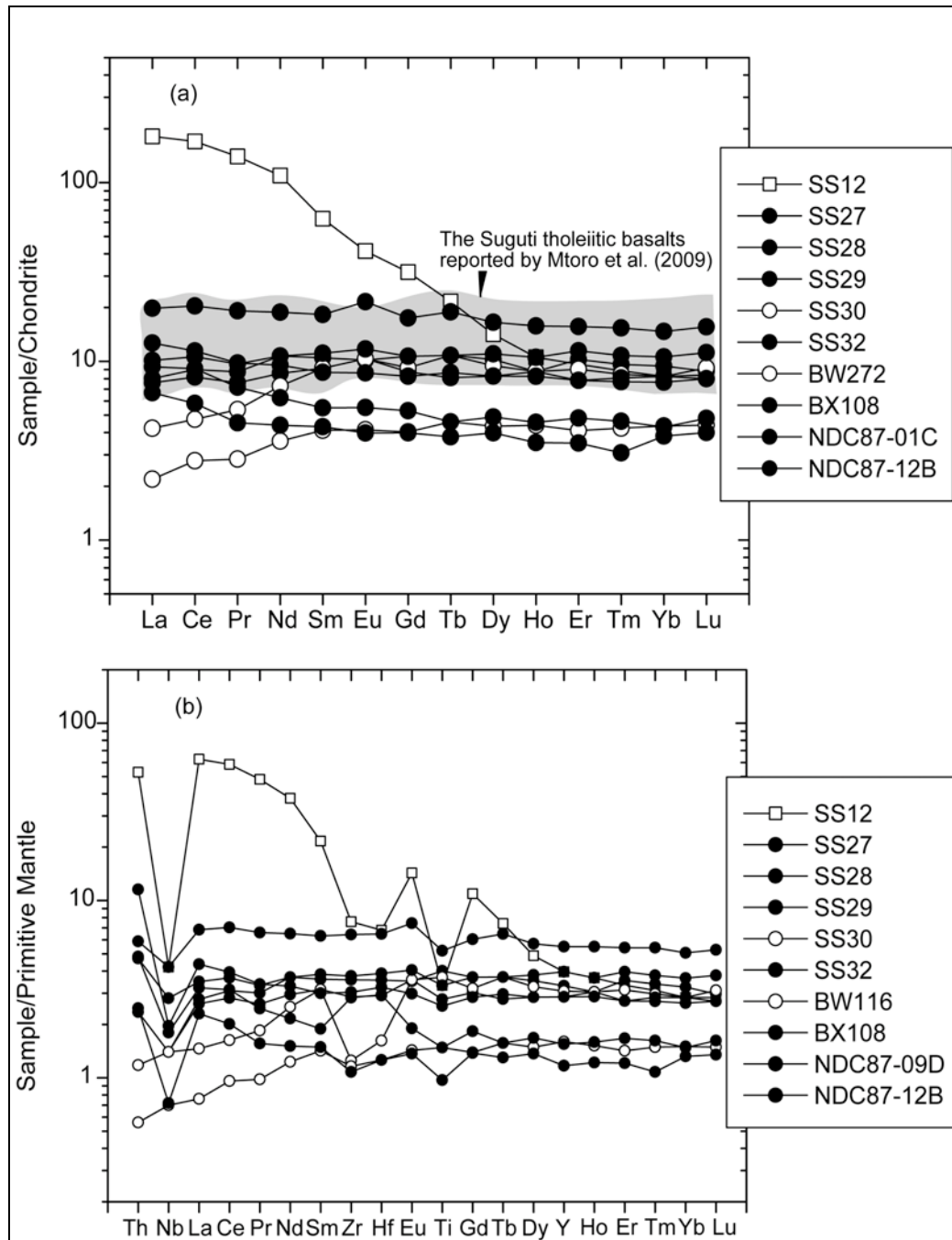


Figure 5: (a) Chondrite –normalized diagram (b) Primitive mantle-normalized diagram for the Simba Sirori – Majimoto segment Mg-rich metabasalts. Normalizing values from Sun and McDonough (1989).

Sm – Nd isotopic composition

The Sm – Nd isotopic data is presented in Table 3. Uncertainties quoted in Table 3 are at 2σ . All six samples define a positively correlated trend in $^{147}\text{Sm}/^{144}\text{Nd} - ^{143}\text{Nd}/^{144}\text{Nd}$ space (Fig. 6), which corresponds to an isochron age of 2777 ± 160 Ma (2σ , MSWD = 4.9) (isochron calculated using the Isoplot program of Ludwig 2003). Ignoring sample SS 29, which is responsible for greater scatter in the regression, results in a statistically indistinguishable but more precise age of 2768 ± 38 Ma (MSWD = 1.2). Calculated initial ϵ_{Nd}

values assuming an igneous crystallization age similar to the isochron age range from +0.66 to +2.81 (Table 3). The 2768 ± 38 Ma age of the Mg-basalts is within error of the 2755 ± 1 Ma reported for the cogenetic tholeiitic basalts and calc-alkaline rhyolites of the Suguti area (Mtoro *et al.* 2009) to the west of the area in the same belt. Thus, the 2768 ± 38 Ma age of the Mg-rich metabasalts of the Simba Sirori – Majimoto segment is interpreted as their emplacement age that is unaffected by crustal material.

Table 3: Sm - Nd isotopic data for the Simba Sirori - Majimoto segment Mg-rich metabasalts

Sample	Sm (ppm)	Nd (ppm)	$^{147}\text{Sm}/^{144}\text{Nd}$	$^{143}\text{Nd}/^{144}\text{Nd}$	$\epsilon_{\text{Nd}} (2.76 \text{ Ga})$
SS 12	10.2	59.8	0.1031	0.511040 ± 3	2.21
SS-27	1.63	4.76	0.2069	0.512920 ± 4	1.88
SS-28	1.28	3.94	0.1963	0.512733 ± 4	2.01
SS-29	2.74	8.87	0.1866	0.512488 ± 4	0.66
SS-30	1.27	3.25	0.2361	0.513501 ± 3	2.81
SS-32	1.65	5.05	0.1974	0.512750 ± 3	1.94

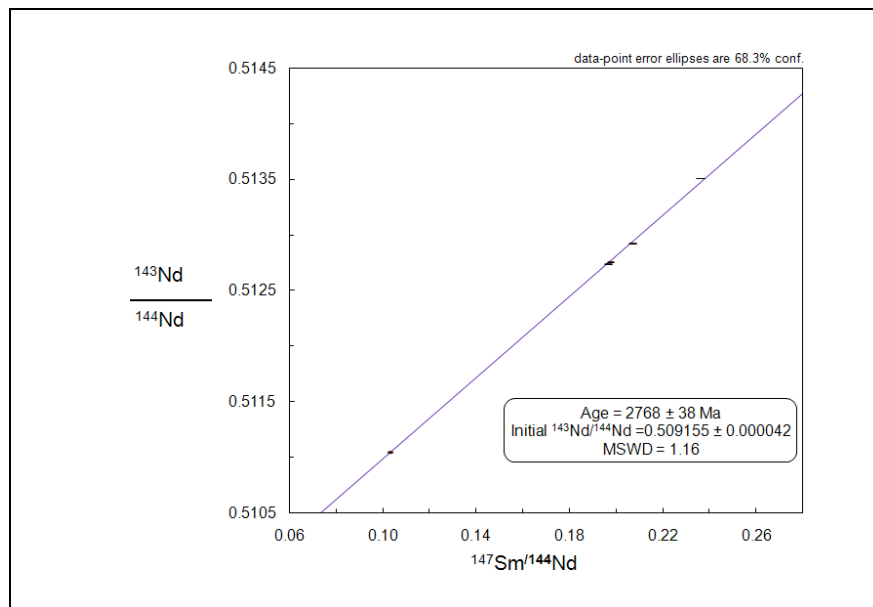


Figure 6: Sm-Nd isochron for the Simba Sirori – Majimoto segment Mg-rich metabasalts

DISCUSSION

The selected Mg-rich metabasalts from Simba Sirori – Majimoto area have MgO contents of up to 16 wt % at a SiO₂ value of 49 wt % and Mg # = 52 – 72. These values are much higher than those of the primitive NMORB (MgO = ~8 wt % and Mg # = 55 at a SiO₂ value of 50 wt%, Sun and McDonough 1989) and are essentially similar to those of the modern ocean plateau basalts (Kerr 2003) and Archaean komatiitic basalts (Shimizu *et al.* 2005, Hollings *et al.* 1999). NMORBs are interpreted to be derived by adiabatic decompression melting of the upwelling upper mantle that is mainly consisting of olivines (Klein 2003). The mantle source of the Simba Sirori –Majimoto rocks, therefore, should be different from that which NMORB is derived and would require a source which could produce more magnesian magmas than the melting of the upper mantle.

Although the MgO contents of the Simba Sirori – Majimoto metabasalts are lower than those of known komatiities (MgO = 30 wt %), they are comparable with komatiitic basalts which, when occur together with komatiites, are often interpreted to have formed by fractional crystallization of the parental komatiite coupled with assimilation of the crustal material (Hollings *et al.* 1999, Shimizu *et al.* 2005). Both the oceanic plateaus basalts and komatiites are considered to be derived from the decompression melting of upwelling hotter mantle known as mantle plumes (Kerr 2003) that start in the lower mantle.

The rocks share some geochemical characteristics with the Suguti tholeiitic basalts reported by Mtoro *et al.* (2009). These features include nearly flat REE patterns (Fig. 5a), negative anomalies of Nb and Ti (Fig. 5b). The later is a diagnostic feature of magmas produced at convergent margins and /or magmas affected by crustal contamination and Mtoro *et al.* (2009)

interpreted the Suguti rocks as having formed at convergent margin with minimal crustal assimilation. Comparing the epsilon Nd value of rocks ($\epsilon\text{Nd} = +0.66$ to $+2.81$ at 2.7 Ga) and the corresponding mantle value at the same time assuming a linear evolution of the mantle ($\epsilon\text{Nd} = 2.2$ at 2.7 Ga, Depaolo 1981) corroborate the earlier inference by Mtoro *et al.* (2009) that little crustal assimilation (indicated by lower ϵNd values of up to $+0.66$) played part in the magmagenesis of these rocks. Contamination of the parental magmas by the felsic crust is further constrained by higher Th/Nb ratios (0.10 – 1.50, mean = 0.39) of the samples than those of NMORB (Th/Nb = 0.05, Sun and McDonough, 1989) but tending to upper crustal Th/Nb ratios of 0.8 (Rudnick and Gao 2003).

The foregoing discussion suggests that the 2.7 Ga Mg-rich basalts of the Simba Sirori area in southern MMGB can be interpreted as being derived by the contamination of the komatiitic magmas by the felsic crust. Such a process was considered to be responsible for the generation of the 2.7 Ga siliceous high magnesium basalt (SHMB), which have SiO₂ = 51 to 55 wt % and MgO = 10 - 16 wt % of Kambalda, Australia (Sun *et al.* 1989, Leshner and Arndt 1995). It should be noted that the inference for the involvement of the komatiitic magmas is from a geochemical point of view but komatiites have not been reported to occur in the Simba Sirori – Majimoto area, nor in all of the greenstone belts of Tanzania. Furthermore, the Simba Sirori – Majimoto Mg-rich metabasalts are the most magnesian basalts to be reported from the Tanzania Craton and although their MgO contents are lower than those of komatiites, they provide a clue to the presence of komatiites in the Archaean craton of Tanzania. Such magnesian lavas are common in other cratons of the world including Barberton of South Africa, Belingwe of Zimbabwe, Superior Province of Canada (Windley, 1995).

ACKNOWLEDGEMENTS

The research work in the geology and mineralization of greenstone belts of Tanzania was financially supported by Sida/SAREC to whom the author is grateful. The reviews and criticism by Dr. Athanas Macheyeky and Dr. Daud Jamal have greatly improved the scientific output of this manuscript and are highly acknowledged.

REFERENCES

- Barth H 1990 Provisional Geological Map of Lake Victoria Gold field, Tanzania 1:500, 000 (with explanatory notes). *Geol. Jahrb.* **B72**: 109-229.
- Borg G and Krogh T 1999 Isotopic age data of single zircons from the Archaean Sukumaland Greenstone belt, Tanzania. *J. Afr. Earth Sci.* **29**: 301-312.
- Borg G and Shackleton RM 1997 The Tanzania and NE Zaire cratons. In: de Wit MJ and Ashwal LD (eds), *Greenstone Belts*. Claredon Press, Oxford, 608-619.
- Campbell IH, Griffiths RW and Hill RI 1989 Melting in an Archaean mantle plume: head it's basalts, tails it's komatiites. *Nature* **339**: 697-699.
- Clifford TN 1970 The structural framework of Africa: In Clifford TN and Gass IG (eds), *African Magmatism and Tectonics*. Oliver and Boyd, Edinburgh, 1-26.
- Cloutier J, Stevenson RK and Bardoux M 2005 Nd isotopic, petrologic and geochemical investigation of the Tulawaka East gold deposit, Tanzania Craton. *Precamb. Res.* **109**: 257-291.
- Condie, K.C., 1997. Plate tectonics and crustal evolution. 4th edition, Butterworth Heinemann, 282 pp.
- DePaolo DJ 1981 Neodymium isotopes in the Colorado Front Range and crust-mantle evolution in the Proterozoic. *Nature* **291**: 193.
- Hollings P, Wyman D and Kerrich R 1999 Komatiite-basalt-rhyolite volcanic associations in northern Superior Province greenstone belts: significance of plume-arc interaction in the generation of the proto continental Superior Province. *Lithos* **46**: 137-161.
- Jensen LS 1976 A new cation plot for classifying subalkalic volcanic rocks. Ontario Division of Mines. *Miscellaneous paper* 66.
- Kerr AC 2003 Oceanic Plateaus. In Rudnick RL (ed), *The crust vol 3, Treatise in Geochemistry*, Elsevier-Pergamon, Oxford, 537 -566.
- Klein EM 2003 Geochemistry of the igneous oceanic crust. In Rudnick RL (ed), *The crust vol 3, Treatise in Geochemistry*, Elsevier-Pergamon, Oxford, 433 - 464.
- Leshner CM and Arndt NT 1995 Trace element and Nd isotope geochemistry, petrogenesis and volcanic evolution of contaminated komatiites at Kambalda, Western Australia. *Lithos* **34**: 127-157.
- Ludwig KR 2003 Users' manual for isoplot/Ex version 2.3. A geochronological toolkit for Microsoft Excel. Berkeley Geochronology Centre. *Special Publication* No. 1a.
- Manya S 2004 Geochemistry and petrogenesis of volcanic rocks of the Neoproterozoic Sukumaland greenstone belt, northwestern Tanzania. *J. of Afr. Earth Sci.* **40**: 269 - 279.
- Manya S 2011 Nd-isotopic mapping of the Archaean-Proterozoic boundary in southwestern Tanzania: implication for the size of the Tanzania Craton. *Gondwana Res.* **20**: 325 - 334.
- Manya S, Kobayashi K, Maboko MAH and Nakaruma E 2006 Ion microprobe zircon U-Pb dating of the late Archaean metavolcanics and associated granites of the Musoma-Mara Greenstone belt, Northeast Tanzania: Implications for the geological evolution of the Tanzania Craton. *J. Afr. Earth Sci.* **45**: 355 - 366.
- Manya S, Maboko MAH and Nakamura E 2007 The geochemistry of high-Mg andesite and associated adakitic magmatism in the Musoma-Mara

- Greenstone Belt, northern Tanzania: possible evidence for Neoproterozoic ridge subduction? *Precambrian Research* **159**: 241 - 259.
- Messo CWA 2004 *Geochemistry of Neoarchaean volcanic rocks of the Ikoma area in the Kilimafedha greenstone belt, Northwestern Tanzania*. M.Sc thesis, University of Dar es Salaam, 101 p.
- Mtoro M, Maboko MAH and Manya S 2009 Geochemistry and geochronology of the bimodal volcanic rocks of the Suguti area in the southern part of the Musoma-Mara Greenstone Belt, Northern Tanzania. *Precambrian Research* **174**: 241 - 257.
- Shimizu K, Nakamura E and Maruyama S 2005 The geochemistry of ultraamafic to mafic volcanic from the Belingwe greenstone belt, Zimbabwe: magmatism in an Archaean Large Igneous Province. *Journal of Petrology* **46**: 2367 - 2394.
- Smithies RH, Champion DC and Sun SS 2004 The case for Archaean boninites. *Contribution to Mineralogy and Petrology* **147**: 705 - 721.
- Rudnick RL and Gao S 2003 Composition of the continental crust. In Rudnick RL (ed), *The crust vol 3, Treatise in Geochemistry*, Elsevier-Pergamon, Oxford, 1 - 64.
- Sun SS and McDonough WF 1989 Chemical and isotopic systematics of oceanic basalts: implication for mantle composition and processes. In: Saunders AD and Norry MJ (eds), *Magmatism in Ocean Basins. Geological Society of London, Special Publication* **42**: 313 - 345.
- Sun SS, Nesbitt RW and McCulloch MT 1989 Geochemistry and petrogenesis of Archaean and early Proterozoic siliceous high-magnesian basalts. In: Crawford AJ (ed), *Boninites. University of Tasmania, Geology Department, Hobart, Tasmania, pp* 148 - 173.
- Thomas CM and Kennedy DC 1965 Geological map and a brief explanation of the geology of Quarter Degree Sheet 13, South Mara. Geological Survey Division, Dodoma.
- Wade FB and Oates F 1938 An explanation of the degree Sheet No. 52, Dodoma. Geol. Survey of Tanganyika. *Short paper* **17**: 1 - 60
- Windley BF 1995 *The Evolving Continents*. 3rd edition, John Wiley and Sons, Chichester, 526 pp.
- Wirth KR, Vervoot JD and Weisberger B 2004 Origin and evolution of the Kilimafedha greenstone belt, eastern Tanzania Craton: evidence from field geology and whole rock geochemistry. *Geological Society of America Abstracts with Programs* **36**: 244.